

Antihydrogen Production within a Penning-Ioffe Trap

G. Gabrielse,^{1,*} P. Laroche,¹ D. Le Sage,¹ B. Levitt,¹ W. S. Kolthammer,¹ R. McConnell,¹ P. Richerme,¹ J. Wrubel,¹ A. Speck,² M. C. George,^{3,4} D. Grzonka,³ W. Oelert,³ T. Sefzick,³ Z. Zhang,³ A. Carew,⁴ D. Comeau,⁴ E. A. Hessels,⁴ C. H. Storry,⁴ M. Weel,⁴ and J. Walz⁵

(ATRAP Collaboration)

¹Department of Physics, Harvard University, Cambridge, Massachusetts 02138, USA

²Rowland Institute at Harvard, Harvard University, Cambridge, Massachusetts 02142, USA

³IKP, Forschungszentrum Jülich GmbH, 52425 Jülich, Germany

⁴York University, Department of Physics and Astronomy, Toronto, Ontario M3J 1P3, Canada

⁵Institut für Physik, Johannes Gutenberg-Universität, D-55099 Mainz, Germany

(Received 6 November 2007; published 18 March 2008)

Slow antihydrogen (\bar{H}) is produced within a Penning trap that is located within a quadrupole Ioffe trap, the latter intended to ultimately confine extremely cold, ground-state \bar{H} atoms. Observed \bar{H} atoms in this configuration resolve a debate about whether positrons and antiprotons can be brought together to form atoms within the divergent magnetic fields of a quadrupole Ioffe trap. The number of detected \bar{H} atoms actually increases when a 400 mK Ioffe trap is turned on.

DOI: 10.1103/PhysRevLett.100.113001

PACS numbers: 37.10.De, 36.10.-k, 41.20.-q, 41.90.+e

A long-term goal of \bar{H} experiments is confining ground-state \bar{H} atoms for precise laser spectroscopy [1]. Only a trap for \bar{H} atoms may allow a small number of such atoms to be used efficiently enough for testing CPT and Lorentz invariance with leptons and baryons [2], and for testing for possible differences in the gravitational force on antimatter and matter [3,4]. Ioffe traps have confined hydrogen atoms [5] for spectroscopy [6]. A key technique, cooling hydrogen atoms via collisions with helium-coated walls, is not available for \bar{H} atoms since they would annihilate. The most straightforward antimatter alternative (Fig. 1) is producing \bar{H} atoms within a Ioffe trap superimposed upon the Penning traps used to store \bar{p} and e^+ , and produce the interactions that form \bar{H} atoms.

A big challenge is that the radial Ioffe field (from race-track coils in Fig. 1) destroys cylindrical symmetry [7]—the symmetry that guarantees stable confinement of charged particles in Penning traps [8]. Some controversy arose about whether \bar{p} and e^+ would thus remain confined long enough to form \bar{H} atoms within a quadrupole Ioffe trap. Could particle loss be avoided at low enough particle densities [7], or is it simply not feasible to produce slow \bar{H} within such traps [9]? If they remain confined, could \bar{p} and e^+ be made to interact to form \bar{H} atoms when the Ioffe trap significantly redirects the normally straight magnetic field lines of a Penning trap (Fig. 2)?

ATRAP settled part of this issue by demonstrating long-time confinement of \bar{p} and e^- (in place of e^+) in the presence of the radial field of a quadrupole Ioffe trap [10]. (Similar confinement was also observed with higher-order Ioffe traps [11,12].) This Letter completes the task by reporting the detection of \bar{H} atoms produced within a quadrupole Ioffe trap, the presence of which

actually increases the number of \bar{H} detected. Crucial elements of this demonstration are short plasmas in a short nested Penning trap, a new method to keep e^+ and \bar{p} interacting in a small volume, and coping with the slow cooling of the e^+ in a 1-T field. The \bar{H} form during the e^+ cooling of \bar{p} in a nested Penning trap [13]. This is the most familiar of the two \bar{H} production methods that have been developed [14,15] because it has produced most of the slow \bar{H} observed so far [16–18]. \bar{H} production within a Penning-Ioffe trap via laser-controlled charge exchange [19,20] also seems promising but has not yet been tried.

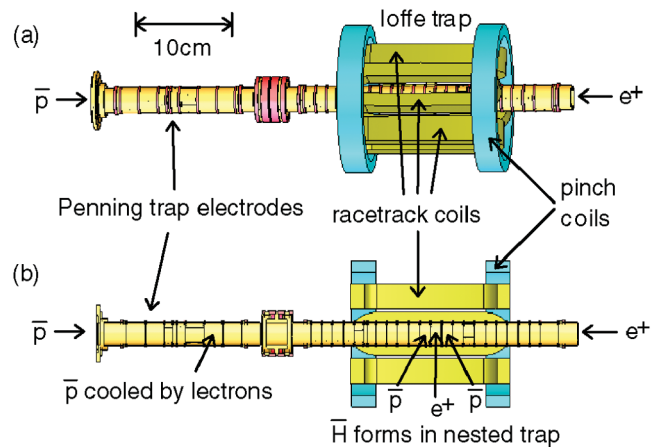


FIG. 1 (color). Outside (a) and cross section (b) views of cylindrical ring electrodes that are biased to form Penning traps for \bar{p} , e^+ , and e^- . In the direction of the central axis (vertical in the experiment) is a 1-T bias field from a solenoid (not shown). The axial and radial fields of a quadrupole Ioffe trap come from two pinch coils and four racetrack coils, respectively.

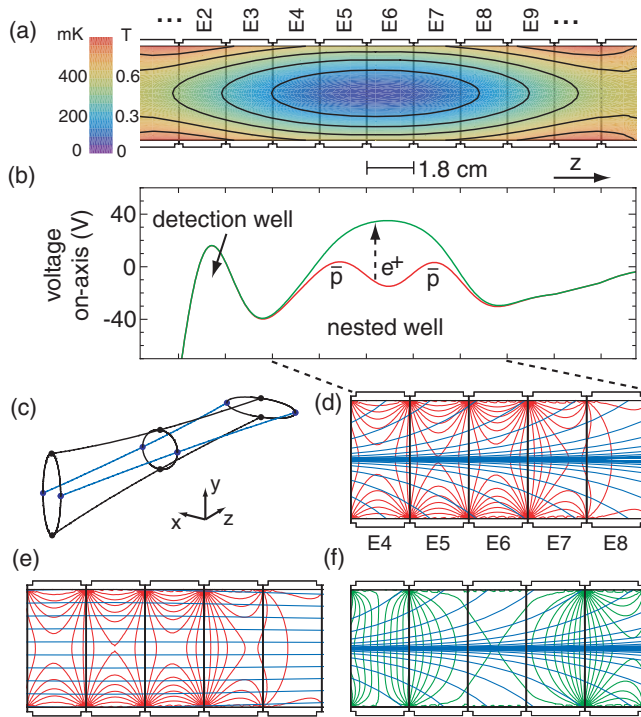


FIG. 2 (color). Cylindrical ring electrodes (black) with well depth contours for ground-state \bar{H} atoms in the Ioffe trap (a). Potential wells seen by charges on-axis (b) during (red) and after (green) \bar{H} production, with corresponding equipotentials for these two cases (d)–(f). An \bar{H} can field ionize and deposit its \bar{p} in the detection well if it travels this direction after production in the nested well. Magnetic field lines (blue) that are parallel to the trap axis with no radial Ioffe field (e) are significantly redirected (c) when the Ioffe field is added (d),(f).

We use \bar{p} accumulation methods [21] now used for all \bar{H} experiments [22]. The unique Antiproton Decelerator (AD) of CERN typically ejects a pulse of 3×10^7 , 5 MeV \bar{p} every 100 s. The \bar{p} slow within a Be degrader and are captured in the lower section of a series of 45 cylindrical, gold-plated copper ring electrodes (Fig. 1), each with an inner radius of $R = 1.8$ cm, with their symmetry axis in the direction of a spatially uniform magnetic field. The \bar{p} cool via collisions with cold trapped photoelectrons that are initially liberated from the degrader by 20-mJ excimer laser pulses at 248 nm [23], and that cool by synchrotron radiation.

The 1-T field used here is lower than the 5-T [16,17] and 3-T [18] used previously for \bar{H} production, since higher fields would greatly reduce the trapping depth for \bar{H} atoms that is shown in Fig. 2(a). The \bar{p} capture efficiency is more than 5 times lower at 1 T than at 3 T, but we still accumulate 30 000 \bar{p} per pulse from the AD, not so different from the capture efficiency reported for \bar{p} accumulated in a smaller trap at a higher field [21].

About 0.6 million \bar{p} have been stacked from successive AD injections [24] at 1 T. The cooling electrons are then

released by removing the \bar{p} trapping potential for a time short enough that they, but not the \bar{p} , leave the trap. Four layers of scintillating fibers and two layers of scintillator paddles detect annihilations of \bar{p} ejected from the trap with high efficiency, and coincidences of these detectors have a higher signal-to-noise ratio. Enough \bar{p} can be accumulated and ejected from the trap to directly measure the charge added to the degrader they strike, but the possible loss of charge due to recoiling nuclei and energetic electrons remains to be studied.

Positrons from a ^{22}Na source are captured after they collide with gas molecules [25] in a separate Penning trap apparatus. Limited experimental space requires that the e^+ travel 7 m through a guide that uses 95 electromagnets to produce and trim a magnetic field along its axis. The guide involves an unusual and abrupt 105° change in direction to redirect a gently rising e^+ trajectory down into the fringing field of the vertical 1-T solenoid, through a 1-mm aperture, to be trapped within the electrodes of Fig. 1. Electron cooling allows efficient e^+ capture [26], typically two e^+ pulses add up to 10 million e^+ for each 100-s AD cycle. The measured charge of e^+ ejected from the trap determines their number, as does the number of counts recorded with the scintillating fibers.

At 1 T the cooling rates are much slower for both the e^- (used to cool \bar{p} and e^+) and the e^+ (used to further cool \bar{p} and to form \bar{H} atoms). In a magnetic field B , e^- and e^+ cool with a time constant no shorter than the $\tau \approx 70(6 \text{ T}/B)^2$ ms for synchrotron radiation to equilibrium with the 7-K trap electrodes. The need to collisionally transfer axial energy to cyclotron energy [27] slows the cooling of the e^- and the e^+ much more. We cope by cooling for 5 to 10 min in deep potential wells, to increase the particle density and collision frequency.

Currents of 80 A in the pinch coils and 69 A in the bars of the racetrack coils (Fig. 1) increase the field to $B_0 = 2.2$ T, produce 375-mK radial and axial well depths for ground-state \bar{H} atoms [Fig. 2(a)], an axial gradient of $\beta = 93$ T/m, and a radial-to-axial field ratio $\beta R/B_0 = 0.78$ (at the trap electrodes). (The trap depth would be 650 mK without the external 1-T bias field.) Multistrand NbTi wire is wound on Ti forms, with close-fitting Ti parts and Al bands containing strong outward forces.

The intricate interplay of trap electrodes, electrostatic equipotentials, and magnetic field lines is represented in Fig. 2. \bar{H} atoms in low-field-seeking ground states see the magnetic equipotentials of Fig. 2(a). The situation is more complex for charged particles which see the potentials shown in Fig. 2(b) and Figs. 2(d)–2(f). The e^+ and \bar{p} interact in the nested Penning trap (red), while the depth of the e^+ well is slowly reduced to prolong the interaction, until no e^+ well remains (green). \bar{H} atoms are detected if they travel to the detection well and are ionized by the high electric fields within this well. Magnetic field lines (blue)

are straight [Fig. 2(e)] until an added radial Ioffe field makes them diverge into electrodes [Figs. 2(d) and 2(f)].

The divergent field lines establish a cutoff radius beyond which no charged \bar{p} or e^+ can be trapped [10] because they are on field lines that terminate on the electrode that must contain them. The cutoff, about 1.2 cm at our full Ioffe field [Fig. 3(a)], decreases with increasing Ioffe trap depth [Fig. 3(b)]. Cooling the charged particles that are within this cutoff is still crucial, to minimize the number lost due to an energy high enough to take them along a magnetic field line to a trap electrode.

To minimize the extent and excursion of \bar{p} and e^+ along the diverging magnetic field lines, we adapt our \bar{H} formation method [16,17] in two ways. First, to make shorter plasmas we use short, radius-length electrodes to form the nested Penning trap. Second, a new method prolongs e^+ and \bar{p} contact with less particle excursion, with less energetic \bar{H} atoms the expected result. As e^+ cool the \bar{p} they start to lose contact. To restore contact, we slowly reduce the depth of the central e^+ well (initially at 0.12 eV/s, slowing to 0.04 eV/s). Figure 2(b) shows the nested Penning trap during (red) and after (green) this reduction.

A typical \bar{H} formation and detection trial starts with 10 min for calibrating the number of e^+ injected into and captured in our trap. Next is 10 min of accumulating and cooling 150 million e^- to use in efficiently capturing e^+ [26], and 400 million e^- for cooling \bar{p} . Over the next 15 min we trap, cool, and accumulate about 0.2 million \bar{p} from 9 injections from the AD, and simultaneously accumulate 60 million e^+ . The \bar{p} and e^+ are transferred adia-

batically (through one electrode at a time by manipulating the potentials applied to the electrodes) from the place where they are initially captured and cooled to electrodes near the center of the deenergized quadrupole Ioffe trap [Fig. 1(b)]. The \bar{p} are injected into the nested trap, the \bar{H} atoms that form as the e^+ initially cool the \bar{p} are discarded, and the scintillating detectors record how many \bar{p} are lost.

After the Ioffe trap is ramped up in 14 min, a detection well [Fig. 2(b)] is created. To make the \bar{p} and e^+ interact to form \bar{H} atoms we lower the depth of the central e^+ well in the nested Penning trap over 11 min. Our measure of \bar{H} production within the Ioffe-Penning trap is the number of produced \bar{H} that travel to the detection well, field ionize due to the large electric fields within, and leave their \bar{p} trapped within this well. The Ioffe field is ramped down in 1 min. The \bar{p} that did not form \bar{H} leave the central green well in Fig. 2(b) to annihilate as the depth of this well is reduced, revealing a distribution [Fig. 3(c)] with a remnant edge from when the Ioffe field caused a radial cutoff. Finally, the detection well depth is zeroed to release the \bar{p} from the \bar{H} that were field ionized and stored earlier in the detection well.

Figure 4(a) shows the number of \bar{H} atoms ionized in the detection well as a function of the depth of the Ioffe trap (given in temperature units for \bar{H} atoms in low-field-seeking ground states). The \bar{H} number is normalized to the average number of \bar{p} participating in \bar{H} production within the Ioffe trap in one of the described \bar{H} production and detection trials. The number of \bar{H} ionized and detected initially decreases with increasing Ioffe trap depth, but is actually enhanced (rather than prevented as some predicted [9]) for a quadrupole Ioffe trap deeper than 300 mK. One possible cause is the radial compression of the e^+ plasma as the Ioffe pinch coils raise the axial magnetic field from 1 to 2.2 T, causing the \bar{p} to interact with a denser e^+ plasma.

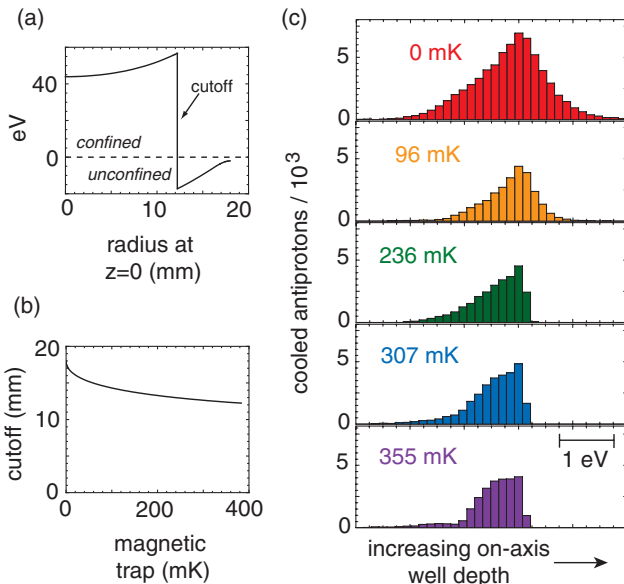


FIG. 3 (color). Illustration of the sharp radial cutoff outside of which no charged particle can be trapped (a), and the dependence of this cutoff upon Ioffe trap depth (b). This cutoff shows up as a sharp edge in the spectrum of \bar{p} released (c) from the green well of Fig. 2(b).

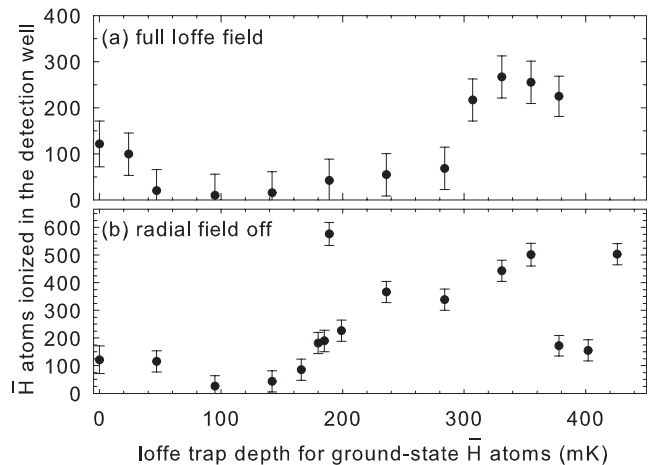


FIG. 4. Number of \bar{H} ionized in the detection well per trial within the Ioffe trap (a) and within only the axial field of the Ioffe trap (b), as a function of the trap depth. \bar{H} numbers are normalized to an average of 0.1 million \bar{p} per \bar{H} production and detection trial, with reproducibility error bars.

To probe the effect of an adiabatic increase in the bias field alone, we repeat the measurements with no radial Ioffe field. The \bar{H} production is higher [Fig. 4(b)], increasing for the strongest fields. About 1% of the \bar{p} lost from the nested trap during \bar{H} production form atoms that we detect, even for the reproducible sharp features in Fig. 4(b) at 200 mK and near 400 mK. These features may represent collective excitations of an adiabatically heated e^+ plasma that enhance or inhibit \bar{p} loss and the proportional \bar{H} production, and they require further study.

Enhanced \bar{H} detection, with up to 1700 \bar{H} atoms ionized in the detection well, takes place when noise is added to heat \bar{p} in the side wells of the nested trap. This extends the interaction of the \bar{p} and the e^+ that cool them, a variation on the driven \bar{H} production method used with no Ioffe trap [17].

The demonstrated production of \bar{H} atoms within a Penning-Ioffe trap opens the way to observing trapped \bar{H} atoms and optimizing their production. The fastest release of trapped \bar{H} atoms comes from ramping the radial Ioffe field off in 1 min, limited by internal quench-protection diodes. A signal equal to our detector background will be produced if 20 trapped \bar{H} atoms/s leave during the Ioffe trap ramp down. A Ioffe trap that can be turned off much more rapidly is under construction.

Significant questions about \bar{H} production remain to be answered when trapped \bar{H} atoms can be detected. First, how many \bar{H} atoms are being produced with low enough energies to be trapped in a 375-mK trap? (A recent reinterpretation [28] of \bar{H} velocity measurements [29] suggests that there should be some.) Second, how many ground-state \bar{H} atoms are being produced? The well depths we quote (e.g. in Figs. 2(a) and 4) are for ground-state atoms, and only highly excited states have yet been identified [17,22]. Third, will some excited states have the right moment to be trapped as predicted [30], and will they stay trapped during cascades to less excited states?

In conclusion, for the first time \bar{H} atoms are produced within a Ioffe trap that is superimposed upon a nested Penning trap. The interaction of \bar{p} and e^+ to form \bar{H} atoms is prolonged with a new method that seems likely to produce lower energy \bar{H} atoms. More \bar{H} atoms are detected within the strong quadrupole Ioffe field, assuaging fears that the Ioffe field would prevent \bar{H} formation. With a Ioffe trap that can be turned off more quickly, it should be possible to look for trapped \bar{H} atoms, and to optimize the production of cold, low-field-seeking, ground-state \bar{H} atoms that can be trapped.

We are grateful to CERN for delivering the 5-MeV \bar{p} from its unique Antiproton Decelerator. This work was supported by the NSF and AFOSR of the U.S., the BMBF, DFG, and Jülich Laboratory of Germany, along with the NSERC, CRC, CFI, and OIT of Canada. G. G. was supported in part by the Humboldt Foundation.

*ATRAP Collaboration spokesperson.
gabrielse@physics.harvard.edu

- [1] G. Gabrielse, in *Fundamental Symmetries*, edited by P. Bloch, P. Pavlopoulos, and R. Klapisch (Plenum, New York, 1987), pp. 59–75.
- [2] R. Bluhm, V. A. Kostelecký, and N. Russell, *Phys. Rev. Lett.* **82**, 2254 (1999).
- [3] G. Gabrielse, *Hyperfine Interact.* **44**, 349 (1988).
- [4] J. Walz and T. Hänsch, *Gen. Relativ. Gravit.* **36**, 561 (2004).
- [5] R. V. Roijen, J. J. Berkhout, S. Jaakola, and J. T. M. Walraven, *Phys. Rev. Lett.* **61**, 931 (1988).
- [6] C. L. Cesar, D. G. Fried, T. C. Killian, A. D. Polcyn, J. C. Sandberg, I. A. Yu, T. J. Greytak, D. Kleppner, and J. M. Doyle, *Phys. Rev. Lett.* **77**, 255 (1996).
- [7] T. M. Squires, P. Yesley, and G. Gabrielse, *Phys. Rev. Lett.* **86**, 5266 (2001).
- [8] T. M. O’Neil, *Phys. Fluids* **23**, 2216 (1980).
- [9] J. Fajans, W. Bertsche, K. Burke, S. F. Chapman, and D. P. van der Werf, *Phys. Rev. Lett.* **95**, 155001 (2005).
- [10] G. Gabrielse *et al.* (ATRAP Collaboration), *Phys. Rev. Lett.* **98**, 113002 (2007).
- [11] G. Andresen *et al.*, *Phys. Rev. Lett.* **98**, 023402 (2007).
- [12] M. Amoretti, C. Canali, C. Carroro, M. Doser, V. Lagomarsino, G. Manuzio, G. Testera, and S. Zavatarelli, *Phys. Lett. A* **360**, 141 (2006).
- [13] G. Gabrielse, S. L. Rolston, L. Haarsma, and W. Kells, *Phys. Lett. A* **129**, 38 (1988).
- [14] G. Gabrielse, D. S. Hall, T. Roach, P. Yesley, A. Khabbaz, J. Estrada, C. Heimann, and H. Kalinowsky, *Phys. Lett. B* **455**, 311 (1999).
- [15] G. Gabrielse *et al.* (ATRAP Collaboration), *Phys. Lett. B* **507**, 1 (2001).
- [16] G. Gabrielse *et al.* (ATRAP Collaboration), *Phys. Rev. Lett.* **89**, 213401 (2002).
- [17] G. Gabrielse *et al.* (ATRAP Collaboration), *Phys. Rev. Lett.* **89**, 233401 (2002).
- [18] M. Amoretti *et al.*, *Nature (London)* **419**, 456 (2002).
- [19] E. A. Hessels, D. M. Homan, and M. J. Cavagnero, *Phys. Rev. A* **57**, 1668 (1998).
- [20] C. H. Story *et al.* (ATRAP Collaboration), *Phys. Rev. Lett.* **93**, 263401 (2004).
- [21] G. Gabrielse, *Adv. At. Mol. Opt. Phys.* **45**, 1 (2001).
- [22] G. Gabrielse, *Adv. At. Mol. Opt. Phys.* **50**, 155 (2005).
- [23] B. Levitt *et al.* (ATRAP Collaboration), *Phys. Lett. B* **656**, 25 (2007).
- [24] G. Gabrielse *et al.* (ATRAP Collaboration), *Phys. Lett. B* **548**, 140 (2002).
- [25] R. G. Greaves and C. M. Surko, *Can. J. Phys.* **74**, 445 (1996).
- [26] ATRAP Collaboration (to be published).
- [27] B. R. Beck, J. Fajans, and J. H. Malmberg, *Phys. Plasmas* **3**, 1250 (1996).
- [28] T. Pohl, H. R. Sadeghpour, and G. Gabrielse, *Phys. Rev. Lett.* **97**, 143401 (2006).
- [29] G. Gabrielse *et al.* (ATRAP Collaboration), *Phys. Rev. Lett.* **93**, 073401 (2004).
- [30] T. Pohl, H. R. Sadeghpour, Y. Nagata, and Y. Yamazaki, *Phys. Rev. Lett.* **97**, 213001 (2006).